# A Model for ß-Amyloid Aggregation and Neurotoxicity Based on Free Radical Generation by the Peptide: Relevance to Alzheimer Disease

K Hensley, JM Carney, MP Mattson, M Aksenova, M Harris, JF Wu, RA Floyd, and DA Butterfield

*PNAS* 1994;91;3270-3274
doi:10.1073/pnas.91.8.3270

*Proc. Natl. Acad. Sci. USA*
Vol. 91, pp. 3270–3274, April 1994
Medical Sciences

# A model for β-amyloid aggregation and neurotoxicity based on free radical generation by the peptide: Relevance to Alzheimer disease

(spin trapping/peptide fragmentation/oxidative stress/enzyme inactivation/membrane damage)

K. HENSLEY*, J. M. CARNEY†, M. P. MATTSON‡, M. AKSENOVA†, M. HARRIS†, J. F. WU†, R. A. FLOYD§, AND D. A. BUTTERFIELD*¶

*Department of Chemistry and Center of Membrane Sciences, †Department of Pharmacology, and ‡Sanders Brown Center on Aging and Department of Anatomy and Neurobiology, University of Kentucky, Lexington, KY 40506; and §Molecular Toxicology Research Group, Oklahoma Medical Research Foundation, Oklahoma City, OK 73104

*Communicated by Earl R. Stadtman, December 8, 1993*

ABSTRACT **β-Amyloid is a 39- to 43-amino-acid neurotoxic peptide that aggregates to form the core of Alzheimer disease-associated senile (amyloid) plaques. No satisfactory hypothesis has yet been proposed to explain the mechanism of β-amyloid aggregation and toxicity. We present mass spectrometric and electron paramagnetic resonance spin trapping evidence that β-amyloid, in aqueous solution, fragments and generates free radical peptides. β-Amyloid fragments, at concentrations that previously have been shown to be neurotoxic to cultured neurons, can inactivate oxidation-sensitive glutamine synthetase and creatine kinase enzymes. Also, salicylate hydroxylation assays indicate that reactive oxygen species are generated by the β-amyloid-(25–35) fragment during cell-free incubation. These results are formulated into a free radical-based unifying hypothesis for neurotoxicity of β-amyloid and are discussed with reference to membrane molecular alterations in Alzheimer disease.**

β-Amyloid peptide (βAP) is a 39- to 43-amino-acid peptide derived from a transmembrane glycoprotein (amyloid precursor protein). βAP forms the core of Alzheimer disease (AD) senile plaques and is postulated to be a major determinant of AD (1–3). In neuronal culture, synthetic βAP forms high molecular mass (>15 kDa) aggregates, disrupts $Ca^{2+}$ homeostasis, and potentiates glutamate excitotoxicity, through processes postulated to involve membrane damage (4). Recent studies indicate that βAP neurotoxicity also may occur independently of excitotoxic amino acids (5).

βAP toxicity appears to be correlated with the aggregation state of the peptide (5, 6). Freshly solubilized synthetic βAP-(1–40) monomer (β1–40) is not toxic to cultured neurons; however, after days of incubation, the suspension becomes toxic (6, 7). In contrast, certain peptide sequences within β1–40, notably β25–35, exhibit rapid aggregation and marked neurotoxicity immediately upon solubilization (7, 8).

No unifying hypothesis has been proposed to integrate the aggregation and neurotoxic properties of βAP into the framework of disparate biochemical aberrations observed in AD (reviewed in ref. 1). We now propose such a hypothesis. We report data that β-amyloid exhibits a chemistry that facilitates the formation of reactive free radical peptides. The results are developed into a free radical model for β-amyloid aggregation and neurotoxicity and are discussed with reference to AD.

## MATERIALS AND METHODS

**Peptides.** Synthetic βAPs were prepared by *t*-butoxycarbonyl (Boc) solid-phase synthesis. Batches of verified purity and neurotoxicity were obtained from Bachem or Athena Neurosciences (San Francisco). Purity was further certified by HPLC-MS of the starting material. β35–25 (the reverse sequence of β25–35) and β25–35(scram) (the scrambled sequence of β25–35) were obtained from Athena Neurosciences. Fatty acid-free bovine serum albumin (BSA) was obtained from Sigma.

**EPR Spectroscopy and Spin Trapping.** βAPs were solubilized to 1.0 mg/ml by addition of buffer [150 mM phosphate-buffered saline at pH 7.4 (PBS) or Hepes at pH 7.4] to lyophilized powder. BSA was solubilized similarly, to concentrations of 1–62 mg/ml. Buffer used for spin trapping contained 50 mM *N-tert*-butyl-α-phenylnitrone (PBN) (Sigma or Aldrich). In studies designed to inhibit putative metal-catalyzed reactions, the chelator deferoxamine mesylate or EDTA (Sigma) was dissolved to 10 mM in PBS/PBN prior to peptide addition. In a further attempt to nullify buffer-borne metals, PBS/PBN was stirred overnight with Chelex 100, a nonspecific metal-chelating agent.

Peptide solutions were aliquoted into a 300-μl aqueous quartz EPR flat cell that was subsequently sealed at both ends and immersed in a 37°C water bath for 0–135 hr and removed periodically for EPR analysis. EPR spectra were acquired on a Bruker (Billerica, MA) 300 EPR spectrometer equipped with computerized data acquisition software. Instrumental parameters were microwave power = 20 mW, modulation amplitude = 0.96 G, gain = $1 \times 10^5$, and conversion time = 10.28 msec. Signal accumulation times were typically 2–5 min. Sample incubated in Hepes buffer utilized a receiver gain of $1 \times 10^6$ and prolonged signal accumulation.

**HPLC-MS Analysis.** Peptide samples were removed from the EPR cell and frozen in liquid $N_2$ pending HPLC-MS analysis. Samples were then thawed and injected into a micro-HPLC system with a 1.0 mm i.d. × 150 mm long Reliasil $C_{18}$ column (Michrom Bioresources, Pleasanton, CA). The column was equilibrated with 100% solvent A (0.1% trifluoroacetate in 2% $CH_3CN$/98% $H_2O$). After injection, two linear gradients were run: 0–20% solvent B (0.07% trifluoroacetate in 90% $CH_3CN$/10% $H_2O$) in 0.04 min followed by 20–56% B in 25 min. Flow rate was 40 μl/min. The absorption of column effluent was monitored at 215 nm. The effluent was fed to an electrospray mass spectrometer (model API III; Sciex, Toronto) operating in the positive ion mode. Measurements were obtained for $m/z$ (mass/charge) values of 200–1400 mass units.

**Glutamine Synthetase (GS) and Creatine Kinase (CK) Assays.** Gerbil cortical homogenate was prepared as described (9) from 3-month-old male mongolian gerbils (Tumblebrook

The publication costs of this article were defrayed in part by page charge payment. This article must therefore be hereby marked "*advertisement*" in accordance with 18 U.S.C. §1734 solely to indicate this fact.

Abbreviations: βAP, β-amyloid peptide; AD, Alzheimer disease; BSA, bovine serum albumin; PBN, *N-tert*-butyl-α-phenylnitrone; GS, glutamine synthetase; CK, creatine kinase; ROS, reactive oxygen species; DHBA, dihydroxybenzoic acid; β1–40, βAP-(1–40).

¶To whom reprint requests should be addressed.

Farms, West Brookfield, MA). β25–35, β35–25, or β25–35(scram) was solubilized in a 1:50 dilution of the cytosolic fraction and incubated for 0–10 min. GS activity was determined by the method of Rowe *et al.* (10) as modified by Miller *et al.* (11) and corrected for nonspecific glutaminase activity by comparison in the presence and absence of ADP and arsenate. CK activity was determined by colorimetry (Sigma kit no. 661).

**Salicylate Hydroxylation.** Generation of reactive oxygen species (ROS) was determined by hydroxylation of salicylate to form dihydroxybenzoic acid (DHBA). β25–35 was preincubated in PBS for 0–3 min after which concentrated sodium salicylate was added to give a final salicylate concentration of 1 mM. The solution was incubated at 37°C for 30 min and then frozen in liquid $N_2$ pending analysis. 2,3- and 2,5-DHBA were measured using HPLC with electrochemical detection as described (12). Salicylate concentration was simultaneously measured with fluorescence detection (300 nm excitation, 412 nm emission), and DHBA was expressed as a ratio to salicylate recovered.

## RESULTS

**Spin-Trapping Results.** In PBN spin-trapping experiments, a nonparamagnetic nitrone (the trap) reacts with a transient free radical (the spin) to produce a stable paramagnetic nitroxide (the spin adduct), which for small radicals yields a six-line spectrum consisting of three doublets. The magnitude of the doublet splittings ($A_H$) depends upon several factors, including the size of the adduct. As the adduct becomes very large, $A_H$ becomes unresolvable because of motional effects, and an apparent three-line spectrum results (13–15).

**β1–40 and β25–35 Spin Trapping.** Fig. 1*A* shows the three-line EPR spectrum acquired from β1–40/PBN after incubation at 37°C in PBS. The isotropic $^{14}N$ nuclear hyperfine coupling in the β1–40-derived spin adduct is obvious from the three-line spectrum; hyperfine coupling to the PBN β-proton was unresolved. A recognizable spectrum first appeared in β1–40/PBN/PBS after a 3-hr incubation at 37°C and reached maximum intensity by 6 hr. No signal was present in PBN/PBS background samples after a 6-hr incubation under the same conditions (Fig. 1*B*). The amyloid-derived signal persisted up to 95 hr of incubation.

In contrast to the 3–6 hr required for β1–40, β25–35 (the toxic 11-amino-acid fragment of the former; sequence GSNKGAIIGLM) showed an EPR signal after only a 3-min incubation at room temperature in PBN/PBS. The β25–35/PBN spectra resembled those of the β1–40 peptide. In the case of β25–35, maximum signal intensity was obtained within a 60-min incubation. Fig. 2 compares early PBN/PBS spectra obtained from β25–35, β1–40, and PBS background. Incubation of β25–35 in unbuffered water also yielded strong EPR spectra within a 3-hr incubation time (data not shown).

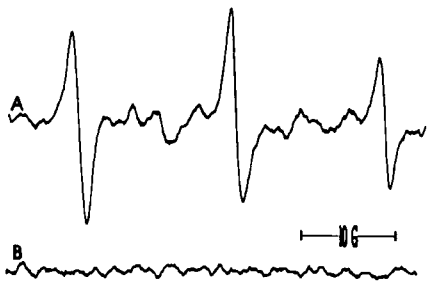


FIG. 1. (*A*) EPR spectrum of β1–40 after 6 hr at 37°C in PBS/PBN. (*B*) EPR spectrum of PBS/PBN after a 6-hr incubation at 37°C (no peptide present).

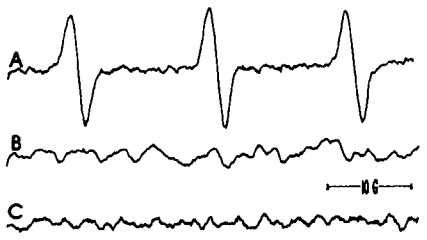


FIG. 2. (*A*) EPR spectrum of β25–35 after a 30-min incubation at 22°C in PBS/PBN. (*B*) EPR spectrum of β1–40 after a 30-min incubation under the same conditions. (*C*) EPR spectrum of PBS/PBN background after a 30-min incubation under the same conditions.

To investigate the role of possible redox-active trace metals in the buffer system, putative metal-catalyzed reactions were inhibited by using Chelex 100 (a nonspecific metal chelator), 10 mM deferoxamine (an iron chelator), or 10 mM EDTA (a divalent cation chelator). In PBS/PBN buffer, all three chelators failed to inhibit the production of a β25–35-derived signal. However, sparging the buffer with $N_2$ did prevent the appearance of the β25–35 EPR signal. In preliminary studies, reoxygenation of the $N_2$-sparged deferoxamine solution caused the appearance of the EPR signal. These results suggest that a reactive amyloid radical was produced by a metal-independent, but oxygen-dependent, mechanism.

β1–40 incubated in Hepes/PBN produced a weak three-line EPR spectrum similar to that produced in PBS (see Fig. 4*C*). In contrast to the PBS buffer, an amyloid-derived signal did not appear in Hepes/PBN until 12–24 hr of incubation at 37°C. The intensity of this spectrum increased linearly up to 95 hr of incubation ($r > 0.95$; data not shown). Incubation with Hepes is complicated by the appearance of significant background (Hepes/PBN) signals at times greater than 36 hr. Fortuitously, the six lines of the Hepes/PBN background signal (tentatively ascribed to trapped Hepes radical) (16) does not overlap the three lines of the amyloid spectrum.

**β35–25, β25–35(scram), and BSA Spin Trapping.** In a preliminary effort to assess the relationship between free radical production and peptide structure, we studied the reverse and scrambled analogues of β25–35, which are not neurotoxic (4). Both the reverse and the scrambled amyloid sequences, when examined after 3 hr of incubation at 37°C in PBN/PBS, produced a detectable EPR signal. As a further control, we studied a large nontoxic protein, BSA. BSA incubated at a concentration equimolar to the βAPs (950 μM) produced no signal before 6 hr of incubation at 37°C, in contrast to β25–35, which showed a strong signal within minutes of incubation at room temperature (Fig. 3). The BSA signal remained approximately constant and much less intense than the amyloid-derived signals throughout the time course of the study (data not shown).

**HPLC-Mass Spectral Analysis.** Fig. 4 presents the chromatograms, mass spectrograms, and EPR spectrum acquired from β1–40 immediately after solubilization or following 135 hr of incubation at 37°C in Hepes/PBN. A Hepes buffer system was chosen because HPLC analysis of PBS-buffered peptide, incubated for even short time periods (<1 hr), was essentially impossible to perform due to the presence of visible aggregates which failed to enter the HPLC column. From the appearance of peaks corresponding to low molecular mass species (Fig. 4*B*), it is evident that β1–40 fragmented during incubation, within the time frame reported to induce neurotoxicity (5). Incubation of β1–40 resulted in a dramatic decrease in the parent peak of the HPLC chromatogram, which was accompanied by the appearance of smaller peptides (Fig. 4 *A* and *B*). Mass spectral analysis of individual

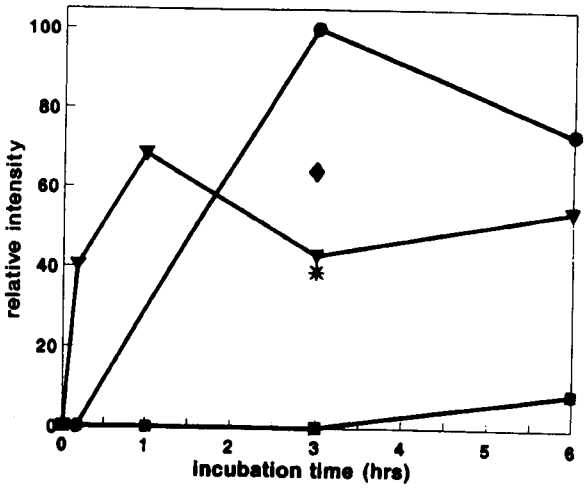


FIG. 3. Comparison of radicalization by β25–35 (▼), β1–40 (●), BSA (■), β35–25 (◆), and β25–35(scram) (*). All peptides were solubilized to 950 μM in PBS/PBN.

peaks from the HPLC column confirmed the mass of the parent peak as β1–40 and indicated the lower masses of the two major peaks of the incubate. Computer simulations of the degradation pattern suggested cleavage at peptide bonds as the most probable mode of peptide breakdown. Based on this assumption, Table 1 presents computer-generated peptide assignments (inclusive of putative PBN spin adducts) for

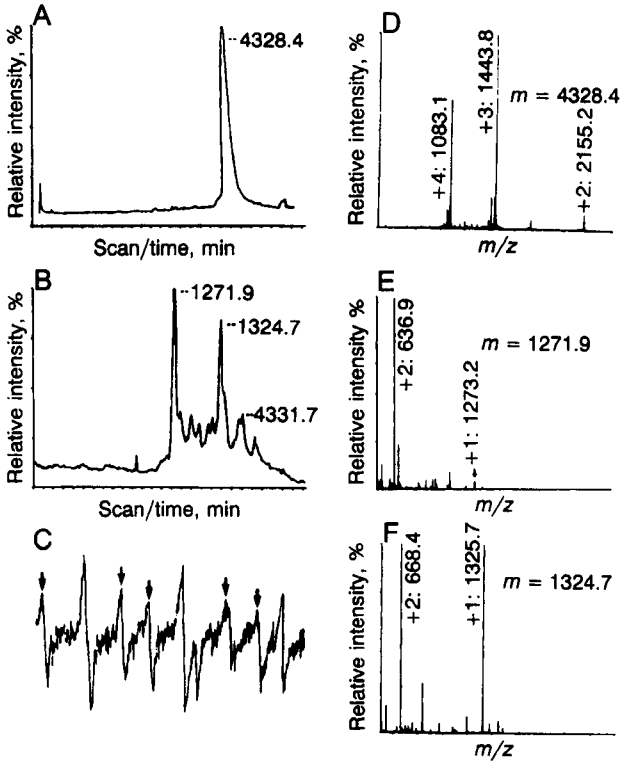


FIG. 4. (*A*) HPLC chromatogram of β1–40 immediately after solubilization in Hepes buffer. (*B*) HPLC chromatogram of β1–40 after 135 hr of incubation in Hepes at 37°C. Numbers beside peaks indicate masses of the principal peak components as measured by MS as described in the text. (*C*) EPR spectrum of β1–40 after 135 hr of incubation at 37°C in Hepes. Arrows show background Hepes signal. (*D*) MS profile of HPLC eluent corresponding to the β1–40 peak shown in *A*. (*E* and *F*) MS profiles of HPLC eluents corresponding to the two major HPLC peaks (mass = 1271.9 and 1324.7, respectively) in *B*.

Table 1. HPLC-MS probable peak assignments

| Actual mass ± SD | Possible species (calculated mass) |
|---|---|
| 4331.69 ± 5.77 | 1–40 (4328.36) |
| 1324.72 ± 0.01 | 23–34 (1322.46) |
| | 26–35-PBN (1324.62) |
| | 29–39-PBN (1322.66) |
| 1271.94 ± 0.36 | 3–11 (1268.26) |
| | 16–25 (1270.39) |
| | 15–22-PBN (1269.49) |
| | 18–26-PBN (1276.39) |
| | 20–28-PBN (1273.38) |
| | 21–30-PBN (1270.37) |

The left-hand column reports the measured masses of major β1–40 peptide fragments. The right-hand column presents the oligopeptide sequences within β1–40 or their putative PBN adducts, which were calculated to lie within ±5 mass units of the measured mass.

these β1–40 breakdown products. Note that most of these assignments contain sequences within the β25–35 region or complementary peptides generated by breakage near the β25–35 termini.

**GS/CK Inactivation.** β25–35 reacted rapidly, in a concentration-dependent fashion, to inactivate both GS and CK enzymes (Fig. 5). Maximum inactivation occurred within 1 min of β25–35 addition; the half-time for this effect was ≈20 sec. Incubation beyond 1 min (up to 10 min) failed to elicit further inactivation of either enzyme, at all peptide concentrations tested. Preincubation of β25–35 for 3–10 min before enzyme addition resulted in loss of the peptide's ability to inactivate GS and CK (data not shown). Neither the reverse β35–25 nor β25–35(scram) could effectively inactivate these enzymes (Fig. 5). Interestingly, BSA was found to protect against β25–35-induced enzyme inactivation (data not shown).

**Salicylate Hydroxylation.** The time course of β25–35-induced ROS production as inferred by DHBA formation was characterized by preincubating solutions of the peptide up to 3 min before addition of salicylate (Fig. 6). β25–35 produced an 85% increase of 2,3-DHBA over that of the buffer control at preincubation times less than 60 sec. The generation of ROS by β25–35 was short-lived and showed little evidence of ROS production when the peptide was preincubated beyond 60 sec (Fig. 6). These results are consistent with the rapid β25–35-induced inactivation of GS and CK (Fig. 5), rapid generation of PBN adduct (Fig. 2), and oxygen dependence of the radicalization reaction (see above).

## DISCUSSION

The data in this paper demonstrate that certain βAPs can generate free radicals in aqueous solution and suggest that radicalization may be a factor in the neurotoxicity of amyloid.

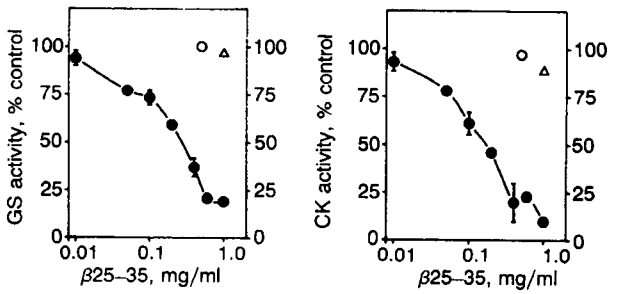


FIG. 5. (*Left*) Profile of GS inactivation by β25–35 (●), β35–25 (○), and β25–35(scram) (△). (*Right*) Profile of CK inactivation by β25–35 (●), β35–25 (○), and β25–35(scram) (△).

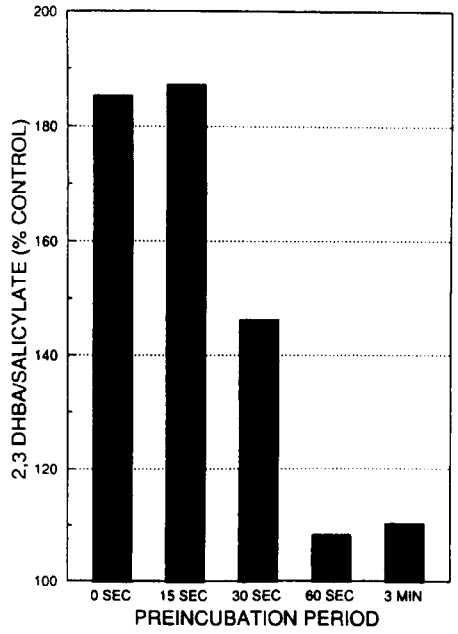


FIG. 6. 2,3-DHBA production as a function of β25–35 preincubation period.

The appearance of an EPR spectrum in PBS/PBN upon addition of βAP clearly indicates the presence of a peptide-derived, free radical species. The motionally unresolved $A_H$ suggests that a sterically bulky moiety has been trapped (13–15). While the mechanism of radicalization is yet unknown, presence of a reactive contaminant is unlikely. HPLC-MS analysis of the original β1–40 indicated a single species of the correct molecular mass, identical to the documentation provided by the supplier. Furthermore, May *et al.* (17) have reported that differences in the neurotoxicity of different synthetic βAP lots were not the result of impurities. Thus, it appears more likely that subtle differences in the solution structure of the peptides determine their relative neurotoxicity.

The kinetic dependence of PBN-adduct generation upon buffer system (PBS vs. Hepes) may be a consequence of the reported ROS scavenging ability of Hepes (16). At 5 mM, Hepes greatly exceeds the molar concentration of βAP used in this study and could effectively interfere with βAP radicalization. Our observation of rapid radicalization by β25–35, in contrast to the lag-time period before β1–40 radicalization, parallels published cell culture data and suggests a novel interpretation. Pike *et al.* (7) reported that β25–35 is neurotoxic immediately upon solubilization, within the time frame that we observed an EPR signal arising from this fragment. However, β1–40 is neurotoxic only after preincubation, which correlates with the lag-time period during which no trapped radical is detected. Thus, it appears that presence of radical species derived from β1–40 (possibly oligopeptides derived from fragmentation reactions) may be necessary for amyloid neurotoxicity.

Although protein damage can result from metal-catalyzed oxidation (7), the inability of metal chelators to inhibit the β-amyloid associated EPR signal reported in this work suggests that metal-catalyzed redox reactions are not operative in our system. Oxygen does seem to be a requirement for radical generation. Furthermore, as indicated by the β25–35-induced formation of 2,3-DHBA (Fig. 6), ROS can be formed as a product of βAP reactions.

Generation of ROS by β25–35 may point to an initiation event expedited by redox-active sulfur. βAP residue 35 is a methionine, a dialkylsulfide. Under appropriate conditions, alkylsulfides react with oxygen in a metal-independent manner to produce a sulfoxide. It is thought that this sulfide oxidation proceeds through a sulfoperoxy radical or persulfoxide intermediate (18). Conceivably, such a reactive intermediate could initiate the type of radical process we have observed with βAP or decay with release of ROS. We therefore suggest that Met-35 may be a key amino acid involved in βAP radicalization, aggregation, and neurotoxicity.

GS and CK enzymes are sensitive to oxidative lesioning and are both affected in AD (9, 19–21). Our data show that β25–35 is a potent inactivator of GS and CK *in vitro*. The rapid enzyme inactivation suggests that the β25–35 sequence can readily attack biological molecules. The observation that β25–35 loses GS/CK toxicity and salicylate hydroxylating potential with preincubation (Fig. 6) parallels the observation of facile PBN-adduct formation by this peptide. Presumably, unstable β25–35 radicals can quickly react with a variety of ambient organic species, other peptides notwithstanding.

The finding that nontoxic βAP fragments (and, at a much slower rate, BSA) generate PBN adducts suggests that radicalization is possibly a necessary but not sufficient criterion for toxicity. Toxicity may be a function of not only the kinetics of radical generation but also the stability of the radical and its efficiency of transfer to lipids and proteins. These characteristics of the radical likely depend on intra- and intermolecular interactions that differ among peptides. Though the chemistry of peptide radicals is essentially unknown, structure–activity precedents from the study of small organic radicals indicate that structure is crucial to radical reactivity. For example, nitrogen- and oxygen-centered radicals are normally very reactive and biologically toxic; however, the presence of sterically bulky or resonance-active ligands adjacent to the radical center (e.g., geminal methyl groups in piperidine nitroxides or a phenyl moiety in PBN spin adducts) converts the radical into an essentially inert species. Indeed, stearate nitroxides and nitrone spin traps have shown promise as antioxidants due to their function as chain-transfer reagents (19, 22). Hence, it is naive to assume that the presence of a radical center should imply biotoxicity independent of other chemical considerations. Thus, while several peptides may generate radicals, the toxicity of a radicalizing peptide depends on a number of factors, and in the case of BSA, it may actually be cytoprotective (see below).

Based on our observations and previously published data, we propose the following model for βAP toxicity. Initial perturbation of proteolytic or other pathways promotes cleavage of amyloid precursor protein and release of βAPs (e.g., β1–40) into the extraneuronal space. Such primary βAPs may then fragment to form smaller, toxic oligopeptide radicals. These radicals could attack cell membranes, initiating lipoperoxidation and damaging sensitive membrane proteins. The membrane barrier function, and ion homeostasis, is compromised. Neurodegeneration follows, possibly expedited by an influx of $Ca^{2+}$. Radical-induced damage to critical glutamate transporters could potentiate glutamate excitotoxicity as has been observed by some researchers (4). βAP-derived peptide radicals could also react with one another or with other proteins to generate covalently bonded aggregates.

Our model for βAP toxicity unifies extant AD data into a coherent theoretical framework. This model is consistent with the slow onset of AD: younger persons may have greater antioxidant capacity and can withstand free radical stress; aging, coupled to environmental insults or genetic defects that depress antioxidant status, could exacerbate consequences of βAP radicalization. The diverse assembly of molecular abnormalities found in AD (23–28) can be rationalized as discreet ramifications of long-term oxidative

stress. Further, our proposed scheme allows the possibility of radical-promoted, protease-independent or protease-dependent cleavage of amyloid precursor protein at a site within the lipid bilayer. Moreover, our hypothesis of free radical-based aggregation and neurotoxicity of βAP offers possible therapeutic strategies in AD involving appropriate free radical scavengers. Finally, our model may help clarify the genesis of prion protein pathology, known to involve amyloid-like plaques and neurodegeneration (29): it is reasonable that mechanisms similar to those developed in this work may be involved in both prion disorders and AD.

The hypotheses presented in this paper, though consistent with much extant AD data, represent only an initial attempt to understand a novel and complex chemistry. Our data underscore the need for further research into the mechanisms of βAP aggregation and neurotoxicity.

We thank Athena Neurosciences for the gift of β35–25 and β25–35(scram) used in these studies. K.H. is an Office of Naval Research Predoctoral Fellow. This work was supported in part by grants from the National Science Foundation (EHR9108764), the National Institutes of Health (AG-10836, AG-09690, NS-23307, and NS-30583), Centaur Pharmaceuticals, the Metropolitan Life Foundation, and the Glenn Foundation for Medical Research.

1. Selkoe, D. J. (1991) *Neuron* **6**, 487–498.
2. Kang, J., Lemaire, H. G., Unterbeck, A., Salbaum, J. M., Masters, C. L., Grzeshik, K. H., Multhaup, G., Beyreuther, K. & Müller-Hill, B. (1987) *Nature (London)* **325**, 733–736.
3. Mattson, M. P., Barger, S. W., Cheng, B., Lieberburg, I., Smith-Swintowski, V. L. & Rydel, R. E. (1993) *Trends NeuroSci.* **16**, 409–414.
4. Mattson, M. P., Tomaselli, K. J. & Rydel, R. E. (1993) *Brain Res.* **621**, 35–49.
5. Busciglio, J., Yeh, J. & Yankner, B. A. (1993) *J. Neurochem.* **61**, 1565–1568.
6. Burdick, D., Soreghan, B., Kwon, M., Kosmoski, J., Knauer, M., Henshen, A., Yates, J., Cotman, C. & Glabe, C. (1992) *J. Biol. Chem.* **267**, 546–554.
7. Pike, C. J., Burdick, D., Walencewicz, A. J., Glabe, C. G. & Cotman, C. W. (1993) *J. Neurosci.* **13**, 1676–1687.
8. Yankner, B. A., Duffy, L. K. & Kirschiner, D. A. (1990) *Science* **250**, 279–282.
9. Oliver, C. N., Starke-Reed, P. E., Stadtman, E. R., Liu, G. J., Carney, J. M. & Floyd, R. A. (1990) *Proc. Natl. Acad. Sci. USA* **87**, 5144–5147.
10. Rowe, W. B., Remzio, R. A., Wellner, V. P. & Meister, A. (1970) *Methods Enzymol.* **17**, 900–910.
11. Miller, R. E., Hadenberg, R. & Gersham, H. (1978) *Proc. Natl. Acad. Sci. USA* **75**, 1418–1422.
12. Floyd, R. A., Henderson, R., Watson, J. J. & Wong, P. K. (1986) *J. Free Radicals Biol. Med.* **2**, 13–18.
13. Janzen, E. G. (1980) in *Free Radicals in Biology*, ed. Pryor, W. A. (Academic, New York), Vol. 4, pp. 115–154.
14. Heller, C. & McConnell, H. M. (1960) *J. Chem. Phys.* **32**, 1535.
15. Butterfield, D. A. (1982) *Biol. Magn. Reson.* **4**, 1–78.
16. Hicks, M. & Gebicki, J. M. (1986) *FEBS Lett.* **199**, 92–94.
17. May, P. C., Gitter, B. D., Waters, D. C., Simmons, L. K., Becker, G. W., Small, J. S. & Robison, P. M. (1992) *Neurobiol. Aging* **13**, 605–607.
18. Liang, J. J., Gu, C. L., Kacher, M. L. & Foote, C. S. (1983) *J. Am. Chem. Soc.* **105**, 4717–4721.
19. Carney, J. M., Starke-Reed, P. E., Oliver, C. N., Landum, R. W., Cheng, M. S., Wu, J. F. & Floyd, R. A. (1991) *Proc. Natl. Acad. Sci. USA* **88**, 3633–3636.
20. Levine, R. L. (1983) *J. Biol. Chem.* **258**, 11823–11827.
21. Floyd, R. A. & Carney, J. M. (1992) *Ann. Neurol. Suppl.* **32**, S22–S27.
22. Miura, Y., Utsumi, H. & Hamada, A. (1993) *Arch. Biochem. Biophys.* **300**, 148–156.
23. Markesbery, W. R., Leung, P. K. & Butterfield, D. A. (1980) *J. Neurol. Sci.* **45**, 323–330.
24. Butterfield, D. A. (1986) *Crit. Rev. Neurobiol.* **2**, 169–240.
25. Selkoe, D. J. (1989) *Annu. Rev. Neurosci.* **12**, 463–490.
26. Ueda, K., Maslia, E., Saitoh, T., Bakalis, L. L., Scoble, H. & Kosik, K. S. (1990) *J. Neurosci.* **10**, 3295–3304.
27. Smith, C. D., Carney, J. M., Starke-Reed, P. E., Oliver, C. N., Stadtman, E. R., Floyd, R. A. & Markesbery, W. R. (1991) *Proc. Natl. Acad. Sci. USA* **88**, 10540–10543.
28. Ginsberg, L., Atack, J. R., Rapoport, S. I. & Gershfeld, N. L. (1993) *Mol. Chem. Neuropathol.* **19**, 37–45.
29. Prusiner, S. B. (1992) *Biochemistry* **31**, 12277–12288.